

# HIGH PRESSURE DIRECT NUMERICAL SIMULATION OF TURBULENT PREMIXED NH<sub>3</sub>/H<sub>2</sub>/N<sub>2</sub> – AIR SLOT FLAME AT $\phi=1.5$

**D. Cecere, M. Cimini, S. Carpenella, E. Giacomazzi**

donato.cecere@enea.it

TERIN-DEC-CCT Laboratory, ENEA, C.R. Casaccia, S.M. di Galeria (Rome), Italy

## Abstract

This study explores the flame dynamics of a premixed NH<sub>3</sub>/H<sub>2</sub>/N<sub>2</sub>-air slot flame at high equivalence ratio and pressure, relevant for clean combustion technologies. The main goal is to shed some light on the interaction between chemical kinetics and turbulent flow structures, providing insights into NO<sub>x</sub> emissions and combustion efficiency. Key findings highlight the effect of the H<sub>2</sub> preferential diffusion on the flame local equivalence ratio, which decreases for negative curvatures, resulting in a NO peak that exceeds the corresponding value in laminar flames. In the post flame zone, the NO concentration is lower than 150 dry-ppm. The results offer critical data for optimizing fuel mixtures and operating conditions in industrial applications to achieve lower emissions and improved performance.

## Introduction

The International Energy Agency (IEA) identifies hydrogen and its derivatives, like ammonia, as carbon-free energy carriers, pivotal in global efforts to decarbonize energy systems [1], and for balancing renewable energy intermittency. To ensure power supply security, gas turbines, known for their electrical efficiency and power density, require fuel-flexible combustion systems to reliably operate with various compositions, including H<sub>2</sub> blends and NH<sub>3</sub>. Despite challenges like low flame speed, NO<sub>x</sub> production [2], stability and reactivity, NH<sub>3</sub> presents advantages over H<sub>2</sub> due to higher density, simpler production, and lower cost-effective energy storage [3]. Due to the convenience of NH<sub>3</sub>, it is often feasible to locally generate the needed H<sub>2</sub> by partially thermally and/or catalytically cracking ammonia, obtaining a NH<sub>3</sub>/H<sub>2</sub>/N<sub>2</sub> blended mixture to be used in combustion systems. In this context, recent findings suggest that adopting a two-stage Rich-Quench-Lean (RQL) strategy enhances flame stability and lowers emissions in ammonia-fired combustors [4]. In fact, in rich-fuel operation, NO<sub>x</sub> emissions are minimized, and excess NH<sub>3</sub> is converted into H<sub>2</sub> via pyrolysis. Then, introducing secondary dilution air downstream allows the remaining H<sub>2</sub> to react under fuel-lean conditions, ensuring low emissions and high efficiency. Moreover, staged combustion under high pressure (> 20 bar) can achieve NO<sub>x</sub> emissions comparable to natural gas turbines [5]. The available literature highlights the role of NH<sub>3</sub> as a potential alternative to replace conventional hydrocarbons in combustion processes. Nevertheless, few

studies have been performed to understand the synergistic interaction between the turbulent flame dynamics and the NH<sub>3</sub> combustion phenomenon. For this reason, this study aims to investigate a rich premixed slot jet flame of NH<sub>3</sub>/H<sub>2</sub>/N<sub>2</sub> at high pressure, by means of Direct Numerical Simulations (DNS), providing a clear understanding of the flame structure, stabilization, and NO<sub>x</sub> formation.

### Case Description and Numerical Setup

This study addresses the resolution of the three-dimensional, reactive, and unsteady compressible Navier-Stokes equations to explore the combustion characteristics of a slot premixed jet flame fueled by an NH<sub>3</sub>/H<sub>2</sub>/N<sub>2</sub> mixture with an equivalence ratio of  $\phi=1.5$ . The fuel mixture is injected through a slot into a co-flow of equilibrium burnt flue gases under a pressure of 25 bar. The mixture composition for the case under investigation consists of 5% NH<sub>3</sub>, 15% H<sub>2</sub>, and 80% N<sub>2</sub> by volume. The co-flow gases have an adiabatic temperature set to 2133 K, while the fuel stream temperature is 750 K, a typical value consistent with the thermal decomposition of ammonia. The co-flow speed is 7 m/s, and the fuel speed is 35 m/s. The Reynolds number of the unburned stream is approximately 41505, resulting in a Kolmogorov scale  $\eta$  around 10  $\mu\text{m}$ . The nominal Karlovitz number (Ka) is 38.92, while the nominal Damköhler number (Da) is 1.43.

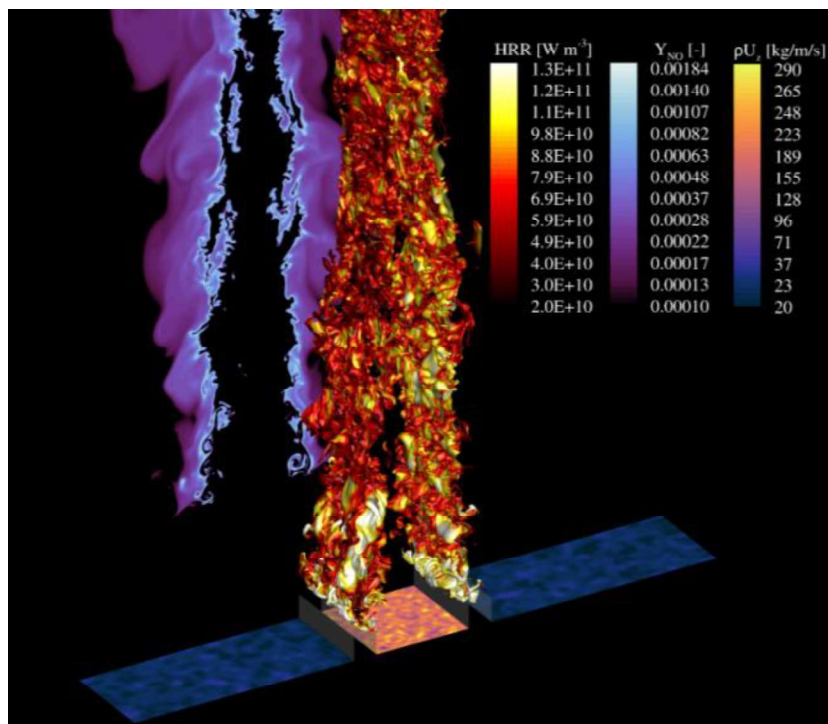


**Figure 1.** Volume rendering of an isosurface of  $T=1500$  K colored with the Heat Release Rate (HRR, black body colormap), NO slice at  $z=0$  (oceanography dense colormap), and momentum fluctuations slices at the slot inlet. Instantaneous taken at  $t=0.0052$  s from the start of the simulation.

The dimensions of the computational domain are  $L_x \times L_y \times L_z = 8.75H \times 6.25H \times H$  in the streamwise (x), crosswise (y), and spanwise (z) directions, respectively. The jet and the coflow are separated by walls of thickness  $H/4$ , similar to the setup used by Luca et al. [6] and Berger et al. [7] in their studies. The final DNS grid consists of  $N_x \times N_y \times N_z = 3000 \times 864 \times 600$  grid points, resulting in approximately 1.55 billion cells.

Jiang's enhanced  $H_2/O_2/N_2$  mechanism, tailored for  $NO_x$  formation in high-pressure  $NH_3$  combustion. Molecular transport in the mixture is modeled using the Hirschfelder and Curtiss expression, considering the Soret thermo-diffusive effect and pressure gradient diffusion. The Wilke's formula for viscosity and the Mathur's expression for the thermal conductivity are used to evaluate mixture-average properties. Preferential diffusion is modelled based on the Hirschfelder and Curtiss law.

The DNS simulation is performed using the ENEA in-house HearT code [8], which exploits a staggered finite-difference scheme to solve compressible, reactive Navier-Stokes equations, with second-order accurate centered diffusive flux calculations and AUSM<sup>+</sup>-up method for convective terms. Extended non-reflecting boundary conditions account for variable transport properties and local heat release. Homogeneous and isotropic turbulence is prescribed in the central premixed jet mixture and coflow burned gases using synthetic generation methods. The flame regime, based on the inlet parameters, falls within the thin reaction zones (TRZ) according to the Borghi-Peters diagram.

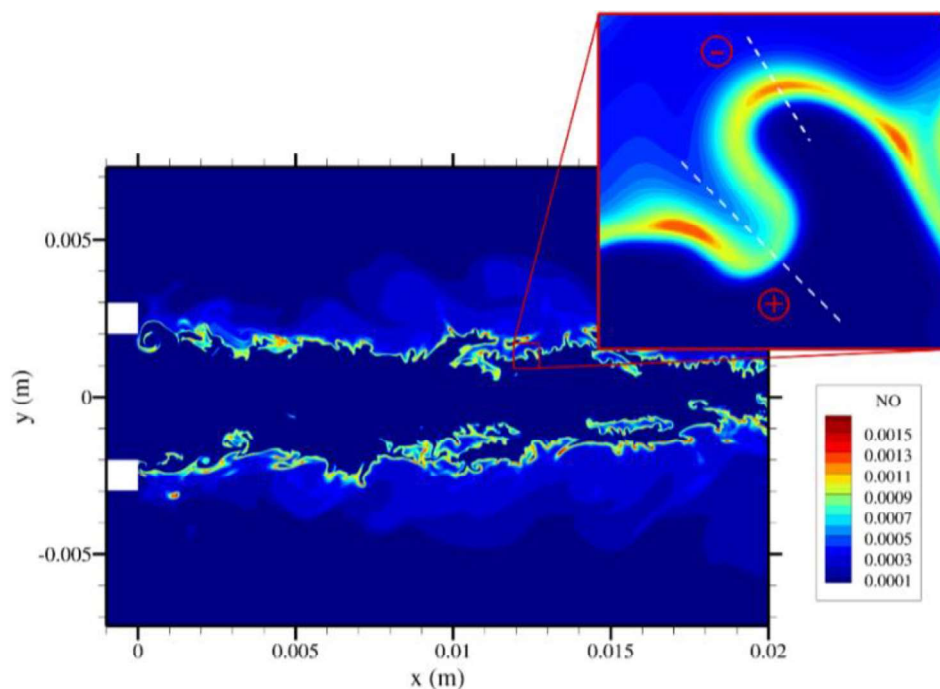


**Figure 2.** Slice at  $z=0$  m and zoomed-in view of  $NO$  mass fraction profile.

## Results

Figure 1 depicts the configuration of the slot turbulent flame and includes an isosurface based on the temperature field, which is color-coded by the HRR. Additionally, it shows a slice at  $z = 0$  illustrating the NO mass fraction and a slice of the momentum x-component at the inlet. Above the duct exit, the flame becomes quickly wrinkled by turbulent vortices, resulting in a prompt increase in fuel consumption due to the enhancement of the flame surface. In this simulation, turbulence plays a key role in the synergistic interaction with the combustion process. When the flame front becomes turbulent it tends to corrugate considerably, generating a chaotic path of alternating positive and negative curvatures. The effect of curvature on combustion plays a crucial role in the NO formation, due to the local enrichment of the mixture that can lead to a decrease in NO and vice versa (the equivalence ratio varies in the range 1.36-1.85 increasing for positive curvatures).

Reaction paths analysis reveals that NO production peaks are located at strong negative curvatures, for values of the local equivalence ratio around 1.4 smaller the nominal one. In these region (for  $c = 0.8$ ,  $c = Y_{H_2O}/Y_{H_2O,Max Lam}$ ) being the progress variable defined with  $H_2O$  mass fraction) the most relevant production rate path is the HNO path. The relevant concentration of OH, O at negative curvature regions promotes their reaction with the high concentration of N radicals (more than 150% greater than positive curvature) to form NO and HNO radicals. The most important path in the NO consumption is the  $N_2O$  and  $N_2$  paths [9].

Inside the flame a continuous region of alternating positive and negative curvatures was chosen for the purpose of analyzing the NO formation behavior (see Fig. 2). A rake line was used to sample the flow field and extract all the major features needed for this analysis from the zones of maximum and minimum curvature.

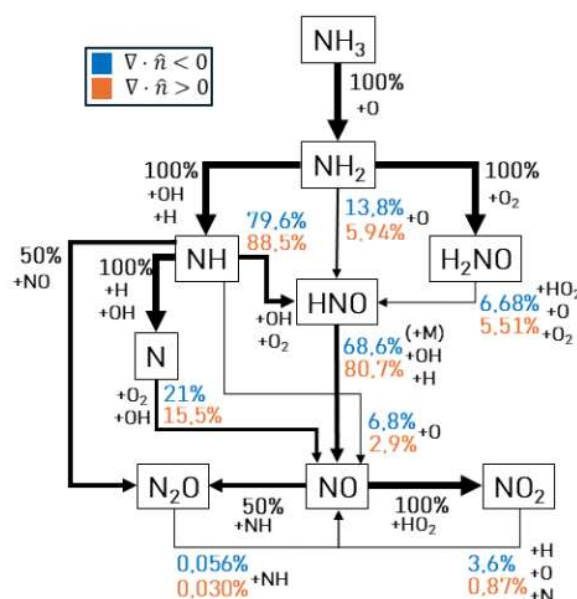


**Figure 3.** Local reaction path diagram of NO formation via N in the flame zone of negative (blue font color) and positive (orange font color) curvature.

The flux diagram in Fig. 3 is evaluated in the local point of maximum curvature (positive and negative) to better describe the NO formation reaction path via N. The diagram also embeds the species involved in every reaction of the pathway, emphasizing the role of the reactions that occur in the process. The results show that, when the curvature is negative, the local production of NO is driven by the HNO decomposition with a third body. This is in agreement with the study of [9], which performed a study of the curvature effects on the NO formation in turbulent  $\text{NH}_3/\text{H}_2/\text{N}_2$ -air premixed flames at 1 atm. The second and third leading mechanism in the formation of NO are due to the reaction of  $\text{O}_2$  with N, and the reaction of H with HNO. Other four reactions that are visible in Fig. 3 contribute in a minor way to the NO production. These are: i) the reaction of OH with HNO; ii) the reaction of H with  $\text{NO}_2$ ; iii) the reaction of O with NH and iv) the reaction of OH with N. When the curvature becomes positive, the major production mechanisms remain unaltered. Nevertheless, the conversion of HNO in the NO production process gains weight, while the conversion of N and NH loses relevance. This behavior can be explained by the fact that zones with positive curvature are affected by a greater  $\text{H}_2$  concentration that reacts, producing  $\text{H}_2\text{O}$  with O and OH favoring their depletion.

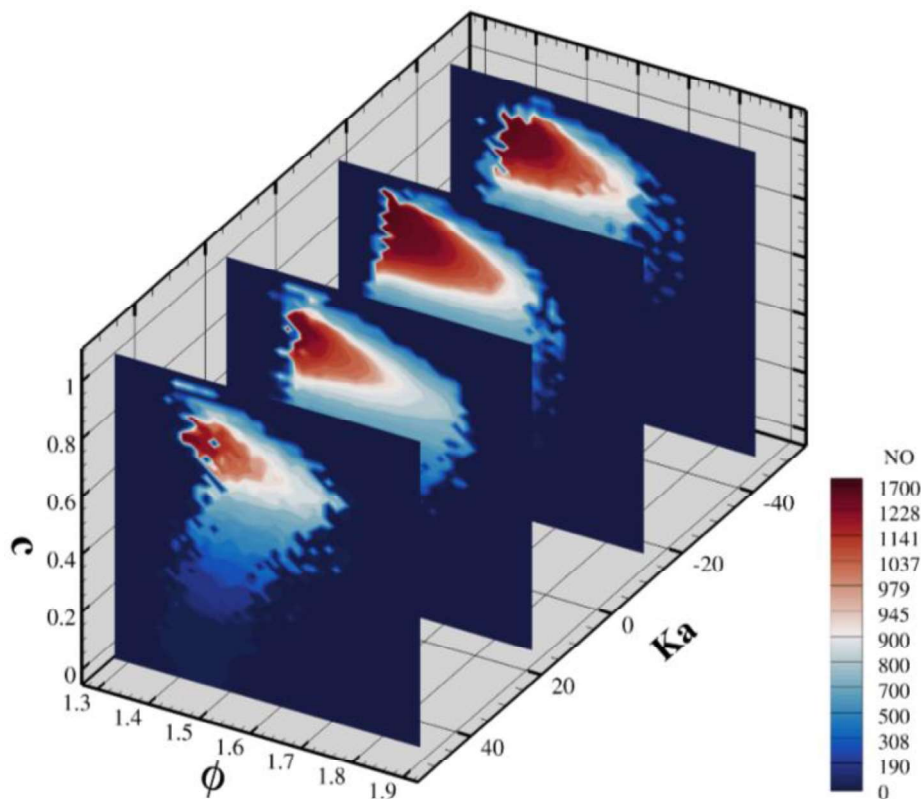


**Figure 4.** Mean NO value (dry-ppm) as a function of  $\phi$ ,  $c$  and the local  $Ka$ .

Figure 4 presents a three-dimensional visualization of the mean NO (dry-ppm) pollutant as a function of  $\phi$ ,  $c$ , and the local  $Ka = (S + S_d \nabla \cdot \hat{n}) \tau_F$ , where  $S$  is the strain,  $S_d$  is the displacement speed,  $\nabla \cdot \hat{n}$  is the curvature, and  $\tau_F = \delta_F / S_L$  the characteristic laminar flame time. The NO maximum values are located for negative

Ka and equivalence ratios less than the nominal one, while on the contrary minimum values are attained for positive Ka and  $\phi > 1.7$ . The NO peaks have been identified, as for the laminar flame, for  $c \approx 0.86$ , a  $c$  value greater than that of the maximum HRR.

In the post flame zone ( $c > 0.9$ ) the NO concentration has a peak around 150 dry-ppm, greater than that of the laminar flame post flame zone ( $< 10$  ppm) since in the latter NO. This is explained by the fact that the laminar flame equilibrium NO values are taken at residence times substantially higher than those in modern gas turbine combustors (where typical values are in the 5-20 ms range).

## References

- [1] International Energy Agency. Global Hydrogen Review. Technical report, IEA, Paris, 2021.
- [2] U.J. Pfahl et al. Combust. Flame, 123:140–158, 2000.
- [3] C. Zamfirescu and I. Dincer. Fuel Process. Technol., 90:729–737, 2009.
- [4] E.C. Okafor et al. Proc. Combust. Inst., 37:4597–4606, 2019.
- [5] S. Gubbi et al. ACS Energy Letters, 8:4421–4426, 2023
- [6] S. Luca et al. J. Prop. Power, 34(1):153 – 160, 2018.
- [7] L. Berger et al. Combustion and Flame, 244:112254, 2022.
- [8] E. Giacomazzi, D. Cecere, M. Cimini, S. Carpenella, Energies, 16, 2023.
- [9] S. Karimkashi et al. Combustion Science and Technology, 1-30, 2023.